Journal of Materials Chemistry C

Accepted Manuscript

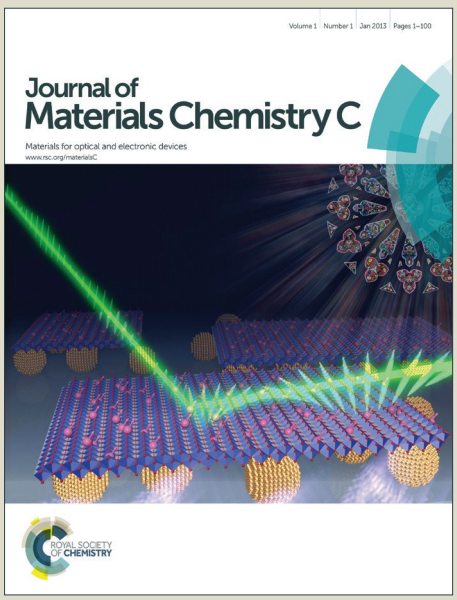

ROYAL SOCIETY OF CHEMISTRY

www.rsc.org/materialsC

Journal Materials Chemistry C

RSCPublishing

ARTICLE

In-situ picosecond transient diffuse reflectance spectroscopy of opaque TiO_2 systems under microwave irradiation and influence of oxygen vacancies on the UV-driven/microwave-assisted TiO_2 photocatalysis

Cite this: DOI: 10.1039/x0xx00000x

Received,
Accepted

DOI: 10.1039/x0xx00000x

www.rsc.org/

Satoshi Horikoshi,[a]*, Hideya Tsutsumi,[a] Hiroyuki Matsuzaki,[b] Akihiro Furube,[b] Alexei V. Emeline,[c] and Nick Serpone [d]*

We report a picosecond transient diffuse reflectance study of commercially available pristine Ishihara ST01 titania, which on treatment with hydrogen gas yields an oxygen-vacancy rich Vo-ST01 system. For comparison, a nitrogen-doped N-ST01 sample was also prepared using urea as the nitrogen donor. These were characterized by XRD and by diffuse reflectance spectroscopy. Transient decay kinetics at 550 nm for all three samples were determined *in-situ* using a 150-ps Nd-YAG pulsed laser system (10 Hz) and a Xe flash lamp (2-μs pulses) probe while samples were being microwave-irradiated (2.45 GHz). The transient(s) absorbing at the probe wavelength displayed double exponential decay kinetics: a ***fast*** decay that occurred within ca. 5–12 ns ascribed to recombination of photogenerated shallow-trapped or free conduction band electrons with valence band holes, and a ***slower*** decay that occurred from hundreds of nanoseconds to several microseconds attributable to recombination of electrons trapped in deep traps (e.g., either as Ti^{3+}or as ***F*** color centers) with free holes. Significant differences were observed for the wet pristine ST01/H_2O and Vo-ST01/H_2O systems when subjected to microwave irradiation; results concurred with those from the degradation of the 2,4-dichlorophenoxyacetic acid (2,4-D) herbicide in aqueous TiO_2 dispersions at 100 ^oC under UV/microwave irradiation (UV/MW) and UV irradiation with conventional heating (UV/CH).

1. Introduction

An essential requirement to examine the dynamics of charge carrier events occurring within semiconductor particles by picosecond and nanosecond time-resolved laser spectroscopy is the availability of stable transparent semiconductor colloidal sols with narrow particle size distribution.[1–3] Such events on TiO_2 aqueous colloidal sols were reported for the first time in the early 1980s by Rothenberger and coworkers[1] who observed a broad transient absorption after 20 ps that was centered at ca. 620 nm and was nearly identical with the broad absorption spectrum of (trapped) electrons produced in acidic (pH 3, λ = 700 nm) and alkaline (pH 10, λ = 780 nm) TiO_2 sols by continuous illumination in the presence of hole scavengers.[4] The rapid appearance of the transient absorption indicated that some of the photogenerated electrons were trapped in less than 20 ps (i.e., within the leading edge of the 30-ps pulse) at Ti^{4+} trapping sites at the particle surface yielding Ti^{3+} species[1] as confirmed by a detailed EPR investigation.[5] Trapping of valence band holes was a much slower process necessitating about 250 ns. A stochastic kinetic model suggested that when the concentration of electron/hole pairs initially formed in the particles was greater than ~ 60, recombination of all charge carriers occurs via a second-order process (ps studies) that was complete in less than 1 ns.[1] However, when the number of electron/hole pairs per particle was low (ns studies; about 6 e^-/h^+ pairs), the model inferred that recombination of charge carriers occurs via a first-order process in which the mean lifetime of a single electron/hole pair was ca. 30 ns, so that trapping of valence band holes could compete with charge carrier recombination. Within this timeframe, trapped holes were somewhat unreactive toward electrons and persisted in the particles for several microseconds.[1] These earlier studies were later supported by femtosecond studies by Furube et al.[6–9] and by Anpo and Takeuchi[10] who observed transient absorption spectra of photogenerated trapped electrons (as Ti^{3+} species) that displayed broad absorption in the range 500–650 nm. Others have also observed broad absorption spectral bands of trapped electrons in TiO_2 albeit at wavelengths between 450 and 800 nm.[11,12]

Assignments of broad absorption bands in the Vis-NIR spectral regions in transient absorption spectral studies of TiO_2 colloids have not been without controversy, however. Henglein et al.[13] assigned the broad absorption band at 400–800 nm with λ_{max} ~ 475 nm in TiO_2 to trapped holes, while a pulse radiolysis study by Serpone and coworkers[14] placed the trapped hole broad absorption at 350 nm. More recent studies by Furube and coworkers[15] observed trapped holes in TiO_2 to display broad bands at ca. 520 and 1100 nm, while trapped electrons displayed broad absorption centered around 770 nm, with the broad absorption of both trapped charge carriers strongly overlapping.[16] In the nanosecond time frame, overlap of absorption bands at 550 nm should be negligible because electron trapping occurs faster (τ ~ 30 ps) than hole trapping by nearly three orders of magnitude (τ ~ 250 ns).[1,11]

The above fundamental studies on charge carrier dynamics notwithstanding, titania systems have received considerable attention in the last three decades as photocatalysts in the remediation of environmental contaminants.[17,18] When such systems are applied to large-scale wastewater treatment systems, photoassisted degradation of the organic contaminants is rather slow.[18] A possible resolution of this issue is to improve the photocatalyst's activity through the

simultaneous use of both UV light and microwave radiation (UV/MW; 2.45 GHz), an integrated methodology proposed as a possible wastewater treatment method.[19–23] The photoactivity of the TiO_2 photocatalyst appears hardly affected when microwave radiation is substituted by conventional heating. Using various approaches, the effects of microwaves, other than thermal, suggested as factors that might affect organic/inorganic reactions, have been examined: for instance, (i) the influence of microwaves (non-thermal effects) on improving the affinity of the TiO_2 surface toward organic pollutants,[24] (ii) the increase in the number of •OH radicals generated by the photooxidation of water,[25] (iii) the influence of the microwave's magnetic and electric fields on photocatalyst activity,[26] and (iv) the enhanced photoactivity of TiO_2 by microwave irradiation under cooling to ambient temperature with the heating attributed not only to a microwave thermal effect, but also to a significant non-thermal effect that implicated hot spots generated on the TiO_2 particle surface.[27]

In the present study we probed the charge carrier dynamics in pristine Ishihara's ST01 titania, in oxygen-vacancy rich ST01 titania (Vo-ST01) and in nitrogen-doped ST01 TiO_2 (N-ST01) under dry and wet (aqueous paste) conditions by *in-situ* picosecond transient diffuse reflectance spectroscopy while the samples were being microwave-irradiated. Results reveal a ***fast*** and a ***slow*** recombination of charge carriers Also investigated were the possible relationships between the presence of oxygen vacancies produced in Ishihara's ST01 titania when pre-treated with hydrogen gas and microwave effects, as the latter might affect the photocatalytic activity of the resulting oxygen-vacancy rich Ishihara ST01 TiO_2 sample (Vo-ST01) toward the photodecomposition of 2,4-dichlorophenoxyacetic acid (2,4-D) in aqueous media when subjected to an integrated UV/microwave irradiation method. Within this context, we examined the pristine ST01 and Vo-ST01 systems and for comparison the photoactivity of the N-ST01 system.

2. Experimental section

2.1 Preparation of TiO_2 particulate specimens

The procedures to prepare hydrogen-treated and nitrogen-doped Ishihara ST01 samples essentially followed the methods reported earlier.[28, 29] For instance, formation of oxygen vacancies in the ST01 titania was achieved by a heat treatment in the presence of hydrogen gas that caused reduction of the ST01 TiO_2 specimen (Ishihara Sangyo Kaisha Ltd.). The titania was placed in a quartz tube (internal diameter, 8 mm) followed by covering the upper and lower ends of the reactor with glass wool. Hydrogen gas was then allowed to flow through the packed TiO_2 particles, followed by heating to 400 ºC for 4 hrs using a heat mantle to yield a TiO_2 powdered specimen henceforth denoted Vo-ST01.

The preparation of N-doped TiO_2 (N-TiO_2) was similar to the procedure used in the synthesis of sulfur-doped TiO_2 with thiourea. Thus, powdered samples of N-TiO_2 were prepared by mixing 1 g of the Ishihara ST01 TiO_2 powder and 2 g of reagent grade urea in a crucible, followed by heating in an electric furnace at 500 °C for 5 hrs (heating rate, 5 °C min^{-1}). Optimal conditions of temperature and mixture ratio were determined in prior exploratory experiments.

Changes in absorption of the UV/Vis light by the TiO_2 samples and their crystalline structures were investigated following absorption of microwave radiation. Changes in the UV/Vis absorption spectra were measured by UV/Vis diffuse reflectance spectroscopy (DRS) using a JASCO V-660 double-beam spectrophotometer equipped with a JASCO ISV-722 integrating sphere unit.

To prepare the samples for this spectroscopic analysis, the pristine ST01 and the oxygen-vacancy rich hydrogen-treated Vo-ST01 powders (30 mg) were added to ultrapure water (30 mL), and were then subsequently UV/CH and UV/MW irradiated with the apparatus illustrated in **Figure 1d** for 1 hr under stirring conditions. Subsequently, the aqueous TiO_2 suspensions were centrifugally separated and then filtered and dried in an electric furnace at 110 ºC, following which the diffuse reflectance spectra were recorded. Note that the organic matter that remains on the TiO_2 surface can frequently cause changes in the absorption spectra. Accordingly, the TiO_2 samples that had been used in the photodegradation of 2,4-D were not used in these experiments.

Crystalline phases (anatase and rutile) and the extent of lattice distortions in the titania systems were determined from X-ray diffraction (XRD) patterns using the PANalytical X'Pert pro XRD apparatus and the Scherer equation.[30]

2.2 Transient diffuse reflectance spectroscopic system

Time-resolved diffuse reflectance measurements were carried out using the second harmonic (532 nm) output pulse from a Nd:YAG laser (Ekslpa, SL311) as the pump light source. The repetition rate of the pump laser was 10 Hz and the pulse duration was ca. 150 ps. About 2-μs pulses from a Xe flash lamp (Hamamatsu, L4642) were used as the probe (~ 5 mm in diameter) light source focused on the sample. A schematic of the overall setup is illustrated in **Figure 1a**. The area investigated by the probe light was within the pump light pulse (~10 mm in diameter). The diffuse-reflected probe light from the sample was then detected with a Si photodiode (New Focus, 1601) after being dispersed by a monochromator (CVI, CM110). Signals from the photodetector were processed with a digital oscilloscope (LeCroy, 6200A) and analyzed with a computer. The risetime of the overall system was about 400 ps. The intensity of the pump light was measured with a pyroelectric energy meter (OPHIR, PE25-SH-V2). All measurements were performed at 295 K. The wavelength of the probe light pulse was set at 550 nm in order to monitor the kinetics of photogeneration and decay of charge carriers in the TiO_2 samples.

Details of the microwave irradiation setup with the single-mode cavity are shown in the photograph of **Figure 1b**; it included a short plunger, an iris, a three-stub tuner, a power monitor and an isolator. The microwave equipment was arranged such that the waveguide was perpendicularly set so as not to interfere with the laser light. The highly precise continuous microwave radiation was generated from a 2.45-GHz microwave semiconductor generator (Fuji Electronic Industrial Co. Ltd.; GNU-201AA; maximal power, 200 W).

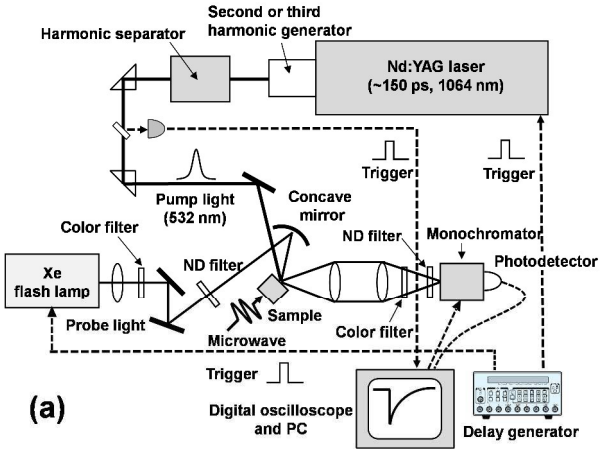

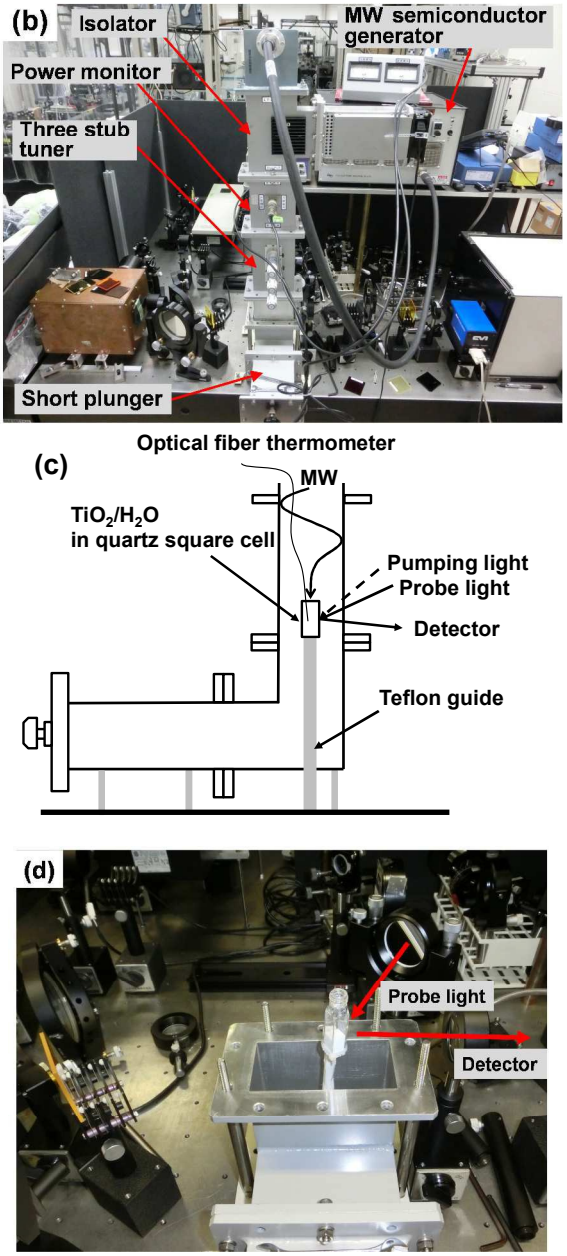

Figure 1. (a) Schematic illustrating the overall diffuse reflectance setup; (b) photograph of the microwave irradiation setup; (c) schematic showing the details the sample area; (d) photograph of the microwave waveguide and sample cell setup.

The short plunger and the single mode cavity were connected to the corner waveguide (**Figure 1c**). The vibration isolation system for the short plunger and the laser were securely fixed. A dry titania sample or a TiO_2/H_2O paste made up with 1.0 mg of TiO_2 and 3 mL of super pure water was introduced into the quartz cell (10 x 10 x 40 mm), which was then positioned and fixed inside the waveguide using a Teflon pole guide. The quartz cell was covered with a Teflon film. The fiber-optic thermometer was introduced into the TiO_2/H_2O sample to monitor any increase of temperature accompanying microwave irradiation. The sample was irradiated with the laser light pulses through the hole vacated on the side of the waveguide, while the diffuse reflected light was monitored through the other hole on the waveguide (**Figure 1d**).

2.3 UV-driven and microwave-assisted degradation of 2,4-D

A 30-mL aqueous dispersion consisting of 2,4-dichlorophenoxy acidc acid (2,4-D; 0.05 mM, pH ~ 5.5) and the TiO_2 powders (loading, 60 mg) was placed in a 150-mL Pyrex glass batch-type cylindrical reactor {Taiatsu Techno Co.; size, 160 mm (height) x 37 mm (internal diameter)} located in the waveguide of the microwave apparatus (**Figure 2**). The reactor was sealed with two Byton O-rings and a stainless steel cap. A pressure gauge and a release bulb were connected to the cover of the reactor. Unless noted otherwise, continuous microwave irradiation was obtained from a Hitachi Kyowa Engineering Co. Ltd. 2.45-GHz microwave generator (maximal power, 800 W) equipped with a power controller, a power monitor, and an isolator (air cooling device). The ca. 39-Watt continuous microwaves emitted from the magnetron were monitored using a power monitor. Temperatures of the aqueous TiO_2/2,4-D dispersions were measured using an Anritsu Meter Co., Ltd. FL-2000 optical fiber thermometer; the dispersion temperature reached a maximum of 101 °C after 9.5 min under microwave irradiation (inset **Figure 2**), and remained constant thereafter to within a 100–101 °C range. The UV source was a Toshiba 75-Watt super high pressure Hg lamp located so as to irradiate the sample reactor through the hole on the side of the waveguide. The dispersion was continually stirred during the irradiation.

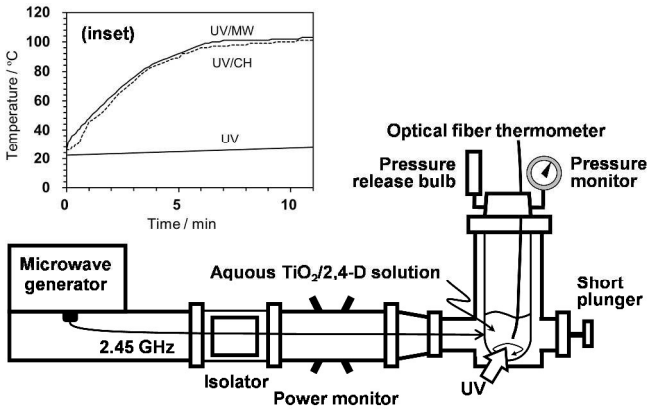

Figure 2. Experimental setup used in the UV-driven and microwave-assisted photodegradation of 2,4-D in aqueous media with TiO_2 dispersions using an integrated UV/MW irradiation method. The inset shows the temperature-time profiles for the UV, UV/CH and UV/MW irradiation of the samples.

The degradation of 2,4-D was examined using three different irradiation methods: (a) UV-driven degradation (UV); (b) UV-driven/microwave-assisted degradation (UV/MW); and (c) UV-driven degradation with conventional heating (UV/CH) at temperatures otherwise identical to those under UV/MW irradiation (ca. 100 °C). In the UV/CH case, a segment of the cylindrical Pyrex reactor was coated with a metallic film, prepared by a metal-organic chemical vapor deposition technique (MOCVD), on one side at the bottom of the reactor to provide the external heat source (applied voltage to metallic film was typically less than 100 V). The uncoated side of the reactor allowed the UV light through. The rate of increase in temperature by the UV/MW route was continually monitored during the irradiation period. The applied voltage on the metallic film was varied so as to obtain a heating rate for the UV/CH method otherwise identical to the heating rate of the UV/MW method as attested to in the inset of **Figure 2**. The dynamics of the degradation process were followed by the loss of UV absorption features of the 2,4-D using a JASCO liquid chromatograph (HPLC) equipped with

a JASCO UV-2070 UV-Vis diode array multi-wavelength detector, and a JASCO Crestpak C-18S column; the eluent was a methanol-water solution (1:2 v/v ratio).

3. Results and discussion

3.1 Characterization of ST01 systems – X-ray diffraction

X-ray diffraction patterns of Ishihara's ST01 anatase titania and of the oxygen-vacancy rich Vo-ST01 samples are displayed in **Figure 3**. The anatase phase was identified from the X-ray peaks at 2θ: 25.31, 37.80, 48.04, 53.89, 55.06, 62.69, 68.77 and 70.29 that accorded with the standard anatase database embedded in the X-ray equipment computer system. The hydrogen gas pre-treatment of ST01 appears to have had no effect on the crystalline form of anatase titania subsequent to formation of oxygen vacancies (Vo).

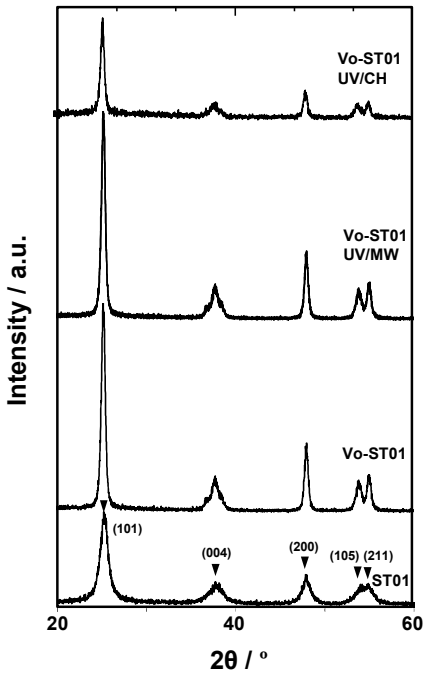

Figure 3. X-ray diffraction patterns of (▼) anatase crystalline phases in the pristine ST01 and Vo-ST01 titania specimens before and after UV/MW and UV/CH irradiation.

The degree of lattice distortions, calculated using the ratio of the standard anatase spectra (database available in the X-ray equipment software) for each of the ST01 systems, were: 0.0018 for pristine ST01 and 0.0002 for the oxygen-vacancy rich Vo-ST01 titania. The degree of distortion for the Vo-ST01 was –0.0003 after being subjected to UV/MW irradiation and 0.0047 when subjected to the UV/CH treatment. Thus, formation of Vo-ST01 titania led to a tenfold decrease of lattice distortion relative to untreated pristine ST01 powder, and even more so after being UV/MW irradiated. Curiously, subjecting the Vo-ST01 system to UV/CH irradiation caused an increase in the extent of distortion. As evidenced in the X-ray diffraction patterns of **Figure 3**, the UV/MW and UV/CH treatments caused no changes in the anatase crystalline phase

3.2 Characterization of ST01 systems – Diffuse reflectance spectroscopy

The UV/Vis absorption spectra, calculated from the diffuse reflectance spectra (DRS), of the ST01 and Vo-ST01 powder samples are displayed in **Figure 4a**, whereas **Figure 4b** displays the difference absorption spectra of Vo-ST01 titania relative to the pristine ST01 TiO_2 and of the Vo-ST01 samples after they had been subjected to UV/MW and UV/CH irradiation. Substantive changes are evident in the spectra of the Vo-ST01 powders at wavelengths longer than the absorption edge of ca. 385 nm when exposed to UV/MW and UV/CH irradiation. In accord with earlier studies by Kuznetsov and Serpone,[31–34] the broad absorption from 370 nm to 700 nm in **Figure 4b** is likely the result of two overlapping absorption bands positioned around 430 nm (~2.90 eV; band AB1) and at ca. 485 nm (2.55 eV; band AB2); it was argued at the time that visible light activation of TiO_2 specimens implicated defects associated with oxygen vacancies that give rise to color centers displaying these absorption bands. [31]

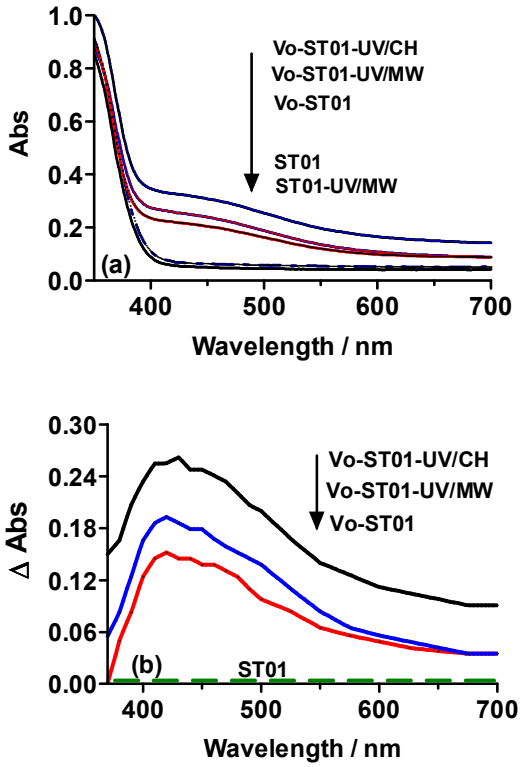

Figure 4. (a) UV/vis absorption spectra of pristine ST01 and Vo-ST01 titania specimens after UV/MW and UV/CH treatment; (b) Difference UV/vis absorption spectra of Vo-ST01 and Vo-ST01 titania specimens after being subjected to UV/MW and UV/CH irradiation relative to untreated pristine ST01 titania.

Although the P25 TiO_2 and the Ishihara ST01 titania have different electronic and structural properties, there are nonetheless some commonalities. In an earlier study on microwave effects on various TiO_2 systems[35] microwave irradiation of H_2-treated and untreated P25 led to an increase of temperature of both particulate systems, albeit each displaying different temperature-time profiles with increasing temperature; the difference was ascribed to different effects on the electronic characteristics of the H_2-treated relative to the untreated P25 TiO_2 particles.

The P25 TiO_2 displayed two discernible bands in the difference diffuse reflectance spectra, one around 400 nm (3.09 eV) and the other at about 365 nm (3.39 eV) together with a broad absorption envelope beyond 420 nm ($h\nu$ < 2.94 eV).[35] The bands at 400 and 365 nm paralleled the spectral variations of the quantum yield (Φ) of photoreduction of O_2 within a spectral range corresponding to the fundamental absorption, which exhibited the typical double-band-

like structure at 385 nm (3.20 eV) and ~340 nm (ca. 3.65 eV)[36] in different heterogeneous systems (liquid-solid and gas-solid) involving pristine undoped TiO_2 samples.[36–38] The origins of such variations have been discussed elsewhere by Serpone[39] and by Kuznetsov and Serpone,[31] who later [34] attributed the broad absorption to formation of Ti^{3+} and ***F*** color centers. By contrast, Lu and coworkers[40] assigned the broad spectral features in the absorption spectrum of a reduced (rutile) TiO_2 single crystal to (Ti^{3+}-V_O) defect centers with the oxygen vacancy V_O located nearest the site of the Ti^{3+} ion.

An alternative view was also proposed[35] that, as demonstrated by Emeline and coworkers[41] for the ZrO_2 system, photoinduced coloration of titania in hydrogen-treated TiO_2s may be caused by photooxidative adsorption of H_2, the first step implicating a reaction with a surface-oxidized oxygen radical anion (O^-•, eqn 1) produced by trapping a valence band hole. Stabilization of this hole state and decrease of recombination of free electrons with this hole state then would increase the number of electron color centers (e.g. ***F*** and Ti^{3+}), with the ***F*** centers being produced by electron trapping into oxygen vacancies.[41] Some of these centers could be thermally ionized by absorption of microwave radiation leading to a greater concentration of free electrons via interaction of the remaining hydrogen atom (eqn 1) with surface oxygen dianions to yield additional free electrons (eqn 2). Thus additional electron color centers can form on trapping the electrons either by oxygen vacancies or by Ti^{4+} species.[42]

$$O^-\bullet + H_2 \rightarrow OH^- + H\bullet \quad (1)$$
$$H\bullet + O^{2-} \rightarrow OH^- + e^- \quad (2)$$

Relevant to the present discussion, recent deep levels transient spectroscopy (DLTS) and thermal admittance spectroscopy (TAS) studies by Arcadipane and coworkers[43] have revealed the presence of no less than four defect levels within the band-gap of TiO_2 located at 0.05 eV, 0.20 eV, 0.42 eV and 1.4 eV below the conduction band, likely connected in one form or other to oxygen vacancies,[44] and ultimately to color centers.

It is curious that absorption at wavelengths above 370 nm for the Vo-ST01 sample following treatment with UV/CH irradiation is more intense relative to the UV/MW-irradiated sample (**Figure 4b**), even though both were subjected to the same temperature conditions (100 ^oC; inset to **Figure 2**). Contrary to conventional heating, which heats up the titania particle from the surface to the bulk, microwave dielectric heating occurs inside-out from the bulk to the surface while the samples were being simultaneously UV-irradiated. Accordingly, it is not unreasonable to infer that the surface of the titania particles was modified, particularly by the former treatment (UV/CH). Hence, to the extent that diffuse reflectance spectra probe the surface of the particles, the greater absorption intensity of Vo-ST01 subjected to UV/CH is sensible. We suppose that a number of defect sites (e.g., anion and cation vacancies; V_a and V_c)[36] were produced at the surface of the titania particles by that treatment as expressed by eqns 3–7:

$$Ti^{4+} + e^- \rightarrow Ti^{3+} \quad (3)$$
$$V_a + e^- \rightarrow F^+ \quad (4)$$
$$Ti^{3+} + \tfrac{1}{2} O_2 \rightarrow Ti^{4+} + O^-_{surf} \quad (5)$$
$$F^+ + \tfrac{1}{2} O_2 \rightarrow V_a + O^-_{surf} \quad (6)$$
$$V_c + h^+ \rightarrow V_S\,(O^-_S) \quad (7)$$

where V_S is a hole color center at the surface and O^-_{surf} denotes surface-trapped holes. The presence of oxygen vacancies within the crystal lattice of ceramics has been reported to enhance microwave heating through Joule heating that bring about changes of the microscopic electrical resistance in ceramics.[45] Although conversion of microwave energy to thermal energy may be affected by the presence of oxygen vacancies, it may be possible (under some conditions) to control the recombination of charge carriers and increase the catalyst photoactivity as inferred in **Figure 5**.[46]

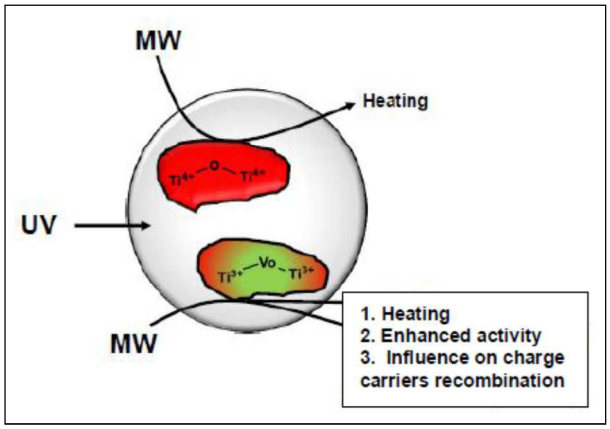

Figure 5. Cartoon depicting the influence of microwave radiation on a regular ST01 particle and on Vo-ST01 particle.

The DRS results of **Figure 4** can be interpreted in terms of the charge conservation law, namely that $[e^-_{tr}] = [h^+_{tr}]$; that is, the number of photogenerated trapped electrons must equal the number of trapped photo-holes. The processes of photogenerated charge carrier trapping can be described by the following set of elementary steps:

$$e^- + V_a \rightarrow F^+\ (Ti^{3+}\text{—}\ V_a) \quad \text{trapping} \quad (8)$$
$$h^+ + F^+ \rightarrow V_a \quad \text{recombination} \quad (9)$$
$$h^+ + V_c \rightarrow V\ (O^-\text{—}V_c) \quad \text{trapping} \quad (10)$$
$$e^- + V \rightarrow V_c \quad \text{recombination} \quad (11)$$

Considering the mechanism of trapping, the charge balance can be expressed by eqn 12 as

$$[e^-_{Va}] + [e^-_{V}] = [h^+_{Vc}] + [h^+_{F}] \quad (12)$$

and the condition $[e^-_{tr}] = [h^+_{tr}]$ can then be represented as (eqn 13),

$$[e^-_{Va}] - [h^+_{F}] = [h^+_{Vc}] - [e^-_{V}] \quad (13)$$

or as (eqn 14),

$$[F^+] = [V] \quad (14)$$

This balance can be considered as resulting from the achievement of quasi-steady-state conditions (eqn 15) realized in the DRS experiments (see **Figure 4**).

$$d[F]/dt = k_8[e^-][V_a] - k_9[h^+][F^+]$$
$$= k_8[e^-][V_{a0}] - (k_8[e^-] + k_9[h^+])[F^+] = 0 \quad (15)$$

so that

$$[F^+] = k_8[e^-][V_{a0}] / (k_8[e^-] + k_9[h^+]) \quad (16)$$

(A similar expression can be written for the trapped holes, which are apparently optically inactive within the experimental spectral range). Thus, the level of UV-induced coloration depends on the concentration of the corresponding defects (e.g. anion vacancies). Accordingly, the increase of the concentration of anion vacancies should result in an increase of photoinduced coloration.

As we noted above, surface reduction with hydrogen leads to formation of both anion vacancies (without trapped electrons) and *F*-type centers (i.e., anion vacancies with trapped electrons, (Ti^{3+}—V_a)). As a result, an extrinsic absorption by *F*-type centers was observed in the diffuse reflectance spectra (**Figure 4**). At the same time, the surface anion vacancies ($V_{a,S}$) can act as adsorption centers for ambient water (eqn 17) that leads to a decrease of the total number of anion vacancies in TiO_2.

$$V_{a,S} + H_2O \rightarrow OH^-_S + H^+_S \quad (17)$$

Sample heating by either microwave or by conventional heating (~100 °C) causes water desorption and restores the surface anion vacancies. Since conventional heating occurs from the surface to the bulk while microwave heating takes place from the bulk to the surface, we expect conventional heating to display a stronger effect on the desorption of surface water and thus on the re-formation of surface anion vacancies. Accordingly, the number of anion vacancies decreases in the order V_O-ST01-UV/CH > V_O-ST01-UV/MW > V_O-ST01; in accordance with eqn 16, the degree of photocoloration should follow the same order.

3.3 Picosecond transient diffuse reflectance spectroscopy

To ascertain the behaviors of the charge carriers (e^- and h^+) we examined next each of the Ishihara ST01 TiO_2 powders by *in-situ* transient diffuse reflectance spectroscopy using 150-ps Nd-YAG laser pulses for excitation (repetition frequency, 10 Hz) and a Xe flash lamp (2-μs pulses) while samples were being subjected to microwave and non-microwave irradiation conditions. At the probe wavelength of 550 nm we probed the photogeneration and decay of trapped electrons[1,47] known to display overlapping absorption bands across the visible to the near-infrared spectral regions owing to formation of photo-induced color centers.[31-34]

Perusal of the decay at the probe wavelength (**Figure 6;** see also **Figure S1** in Supplementary Information) that pertains to recombination of photogenerated charge carriers shows that recombination follows ***fast*** and ***slow*** decay kinetics. Accordingly, the data were analyzed by double exponential kinetics, the data for which are collected in **Table 1**. The ***faster*** decay occurring within 5–12 ns is likely the result of recombination of shallow-trapped (or free) electrons with valence band holes, whereas the significantly ***slower*** decay originates with recombination of deeply-trapped electrons (e.g., as Ti^{3+} and/or as ***F*** color centers on trapping electrons by oxygen vacancies, Vo) with free valence band holes, although our data do not preclude recombination with trapped holes.

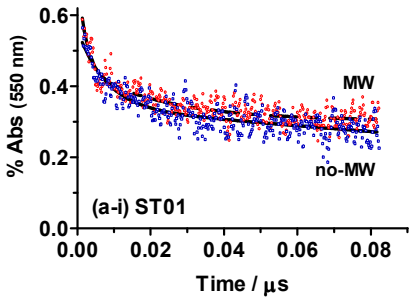

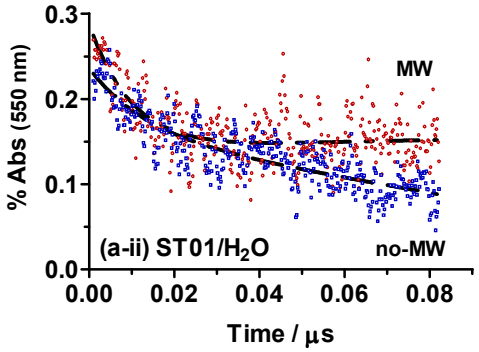

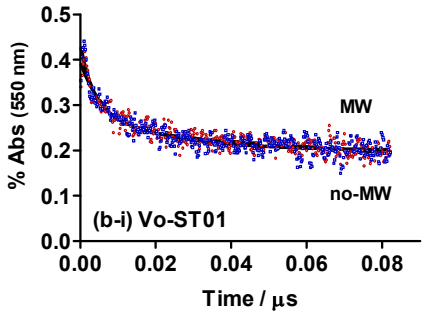

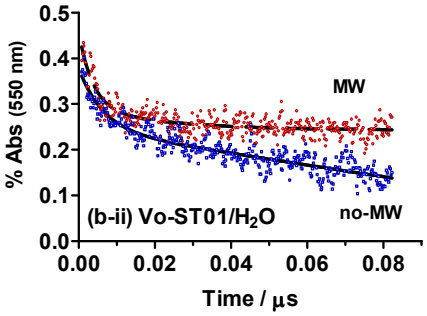

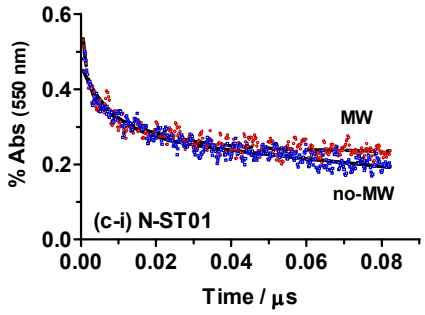

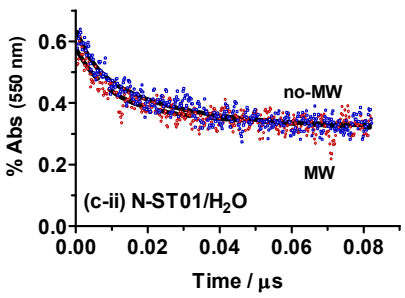

Figure 6. Decay of transient absorption with and without microwave irradiation; (a-i) dry pristine ST01; (a-ii) wet pristine ST01 paste; (b-i) dry Vo-ST01; (b-ii) wet Vo-ST01 paste; (c-i) dry N-ST01; (c-ii) wet N-ST01 titania paste.

Table 1. – Decay of the percent absorption (i.e. recombination kinetics of charge carriers) of various Ishihara ST01 titania systems as dry powders and as aqueous pastes with (MW) and without (no-MW) being microwave-irradiated. Decay kinetics were probed at 550 nm in the region where electrons display significant absorption. Highlighted are the systems where significant differences are observed in the decay kinetics.[a]

TiO_2 systems	Recombination dynamics and decay times of charge carriers			
	k_{slow} (10^6 s^{-1})	k_{fast} (10^8 s^{-1})	τ_{slow} (µs)	τ_{fast} (ns)
ST01 (no-MW)	3.2 ± 0.4	1.6 ± 0.2	0.31	6
ST01 (MW)	2.4 ± 0.3	1.5 ± 0.1	0.42	7
Vo-ST01 (no-MW)	2.5 ± 0.3	1.7 ± 0.1	0.40	6
Vo-ST01 (MW)	2.9 ± 0.2	1.7 ± 0.1	0.34	6
N-ST01 (no-MW)	5.3 ± 0.3	1.5 ± 0.1	0.19	7
N-ST01 (MW)	3.1 ± 0.2	2.1 ± 0.1	0.32	5
ST01/H_2O (no-MW)	***9.1 ± 0.7***	***1.6 ± 0.4***	***0.11***	***6***
ST01/H_2O (MW)	***(<< 0.1)***	***0.93 ± 0.15***	***(>> 10)***	***11***
Vo-ST01/H_2O (no-MW)	***7.4 ± 0.4***	***1.8 ± 0.3***	***0.14***	***6***
Vo-ST01/H_2O (MW)	***0.99 ± 0.27***	***1.7 ± 0.2***	***1.00***	***6***
N-ST01/H_2O (no-MW)	1.8 ± 0.5	0.85 ± 0.09	0.54	12
N-ST01/H_2O (MW)	2.1 ± 0.4	1.1 ± 0.1	0.48	9

[a] Note that all experimental data in this table and in **Figures 6** represent the average of no less than four different experiments.

Except for the nitrogen-doped ST01 (**Figure 6c-i** and **Table 1**) in the dry state, the pristine ST01 (**Figure 6a-i**) and oxygen-vacancy rich Vo-ST01 (**Figure 6b-i**) powdered samples displayed no significant differences in transient decay, regardless of whether or not the samples were microwave-irradiated (see **Table 1**). Note that a temperature increase of about 5–8 ºC for each TiO_2 sample occurred by irradiation with microwaves after ca. 1 min indicating that indeed the samples were microwave-irradiated. For the nitrogen-doped ST01 system, microwave irradiation tended to decrease the slower decay kinetics nearly twofold: k_{slow} = 5.3 x 10^6 s^{-1} *versus* 3.1 x 10^6 s^{-1} reflected in the decay times τ_{slow} = 0.19 µs *versus* 0.32 µs. The ***fast*** decay kinetics were nearly identical within experimental error in all the above cases whether or not the systems were microwave-irradiated.

The ***slow*** decay was particularly interesting as significant differences were observed in the decay times, especially for the aqueous titania pastes, although this assertion precludes the N-ST01/H_2O system, which displayed no significant variances with or without being microwave- irradiated (see **Figure 6c-ii** and **Table 1**). By contrast, paste samples of both the ST01/H_2O and the oxygen-vacancy rich (H-treated) Vo-ST01/H_2O displayed substantial variations between being (MW) and not being (no-MW) microwave-irradiated; particularly significant was the former system (**Figure 6a-ii** and **Table 1**). Indeed, when the ST01/H_2O titania was microwave irradiated the decay kinetics decreased dramatically: k_{slow} = 9.1 x 10^6 s^{-1} (no-MW) *versus* << 0.1 x 10^6 s^{-1} (MW); decay times τ_{slow} = 0.11 µs *versus* >> 10 µs, respectively. The already oxygen-vacancy rich Vo-ST01/H_2O system displays a lesser but nonetheless significant decrease in absorption decay upon being microwave-irradiated: k_{slow} = 7.4 x 10^6 s^{-1} (no-MW) *versus* 0.99 x 10^6 s^{-1} (MW); τ_{slow} = 0.14 µs *versus* ca. 1.00 µs, respectively. Such differences may be due to microwave non-thermal factors for both ST01/H_2O and the oxygen-vacancy rich (H-treated) Vo-ST01/H_2O systems, yet non-thermal factors had no influence on ST01 TiO_2 toward the photodegradation of 4-chlorophenol.[28] Microwave radiation also seemed to have had no effect on the photocatalytic performance of N-doped ST01 TiO_2 (N-ST01).[28]

The kinetics of the processes described by equations 8–11 for *F*-type centers were represented by eqn 15,

$$d[F]/dt = k_8 [e^-] [V_a] - k_9 [h^+] [F^+]$$
$$= k_8 [e^-] [V_{a0}] - (k_8 [e^-] + k_9 [h^+]) [F^+] \quad (15)$$

and depend on the concentration of the defects, on the corresponding rate constants of charge carrier trapping, and on the time evolution of the concentrations of the charge carriers (electrons and holes – eqns 18 and 19, respectively).

$$d[e^-]/dt = - k_8 [e^-] [V_a] - k_{11} [e^-] [V] \quad (18)$$

$$d[h^+]/dt = - k_{10} [h^+] [V_c] - k_9 [h^+] [F^+] \quad (19)$$

Thus, any additional factors that affect the evolution of the charge carrier concentration will also affect the kinetics of the absorption by color centers.

Interestingly, adsorbed waters can also act as hole traps (eqn 20)

$$H_2O_s + h^+ \rightarrow OH^\bullet + H^+ \quad (20)$$

followed by recombination with electrons (eqn 21),[48]

$$OH^\bullet + H^+ + e^- \rightarrow H_2O_s \quad (21)$$

Therefore, the adsorbed waters can create a new (probably) slower channel for charge carrier recombination that changes the kinetics of the absorption decay. At the same time, microwave irradiation can result in the desorption of water from surface anion vacancies, as a result of which the kinetics of absorption decay through the newly re-formed surface defects then become similar to those observed for the un-wetted surface. In turn, it is known the N-doping causes the stabilization of anion vacancies and of the corresponding color centers.[49,50] Accordingly, N-doping results in the formation of a larger number of anion vacancies in the bulk of N-doped TiO_2, and therefore the kinetics of absorption decay do not depend greatly on surface hydroxylation. In fact, the kinetics are more likely dictated

by the rate constants of charge carrier trapping by the bulk defects stabilized by the N-dopant.

3.3 Influence of oxygen vacancies in the photodegradation of 2,4-D

The picosecond results pertaining to the aqueous pastes (**Table 1** and **Figure 6**) should provide some expectations as to the dynamics of degradation of the 2,4-D on the basis that the longer the decay times are (**Table 1**), that is the slower charge carrier recombination is, the faster the degradation reactions should be inasmuch as they can then compete more effectively with recombination processes. In this regard, the data for the ST01/H_2O and Vo-ST01/H_2O (with and without MW irradiation) is most appropriate as they are the data that show the greatest variations in the slow recombination dynamics of the charge carriers. These dynamics are slowest when the specimens are subjected to microwave irradiation: decay times, >>10 μs (MW) *versus* 0.11 μs (no-MW) for ST01/H_2O, while for Vo-ST01/H_2O decay times were 1.0 μs (MW) *versus* 0.14 μs (no-MW), and for N-ST01 0.32 μs (MW) *versus* 0.19 μs (no-MW). Hence for pristine ST01, Vo-ST01, and N-doped ST01 titania the degradation of 2,4-D in aqueous media should be faster under UV/MW irradiation than under UV irradiation alone, or more appropriately under UV/CH irradiation conditions for identical temperatures (100 °C; see insert **Figure 2**). As we shall see below, these expectations are borne out by the time profiles of the photodegradation of 2,4-D in aqueous dispersions of pristine ST01 TiO_2, Vo-ST01 titania and N-doped ST01 titania, displayed in **Figure 7**, and by the dynamics (initial rates) reported in **Table 2**.

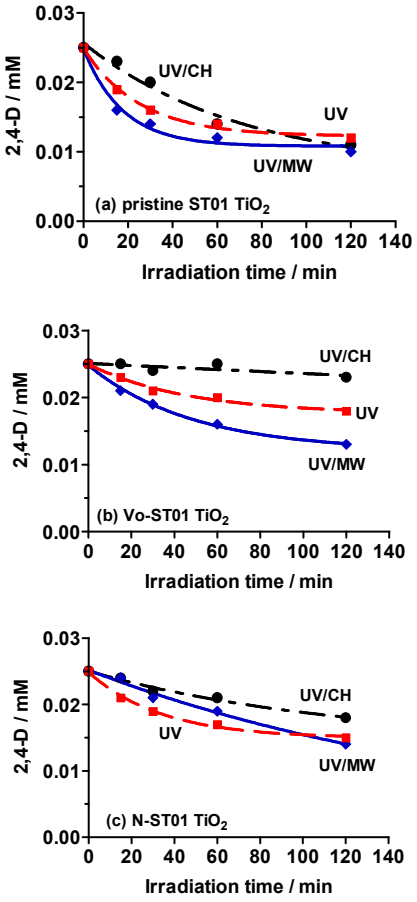

Figure 7. Photodegradation of 2,4-D using UV, UV/MW, and UV/CH irradiation methods: (a) pristine ST01 titania; (b) Vo-ST01 titania with oxygen vacancies, and (c) nitrogen-doped ST01. The UV light irradiance at 360 nm was ca. 0.4 mW cm^{-2}; temperature under UV/MW and UV/CH was 100 °C, whereas temperature was ambient under UV irradiation alone (see insert to **Figure 2**).

Significant differences in the photoassisted degradation of 2,4-D by Vo-ST01 titania samples (**Figure 7b**) are evident relative to pristine ST01 (**Figure 7a**) and N-doped ST01 systems (**Figure 7c**). For pristine ST01, the degradation of 2,4-D under UV/MW irradiation at 100 °C was ca. 25 % faster relative to UV irradiation alone (**Table 2**, **Figure 7a**), likely due to a microwave thermal effect as in the latter case the temperature was ambient. On the other hand, degradation was twofold faster under UV/MW irradiation relative to UV/CH irradiation both occurring at 100 °C (**Table 2**), in fair agreement with earlier results on the degradation of 4-chlorophenol,[29] and in accord with expectations from the picosecond results (**Table 1** and **Figure 5a-ii**).

Table 2. – Dynamics (initial rates) of the photodegradation of 2,4-dichlorophenoxyacetic acid in aqueous media under UV, UV/MW, and UV/CH irradiation; initial concentration of 2,4-D was 0.025 mM; the temperature of the photodegradation under UV/MW and UV/CH conditions were identical.

Titania systems	**Photodegradation dynamics of 2,4-D (x 10^{-4} mM min^{-1})**		
	UV [a]	**UV/MW** [b]	**UV/CH** [b]
pristine ST01	3.0	3.7	1.7
Vo-ST01	0.82	***1.4***	***0.019***
N-doped ST01	2.0	1.3	1.0

[a] ambient temperature; [b] temperature was 100 °C

For the hydrogen-treated ST01 TiO_2 that resulted in the formation of a number of oxygen vacancies, the initial rate of degradation of 2,4-D was nearly twofold faster for Vo-ST01 TiO_2 dispersions under UV/MW (100 °C) relative to UV irradiation alone at ambient temperature (1.4 x 10^{-4} mM min^{-1} *versus* 0.82 x 10^{-4} mM min^{-1}, respectively; **Table 2**), a result due to microwave thermal effects. Most significant were the faster degradation dynamics under UV/MW irradiation relative to UV/CH by nearly two orders of magnitude (1.4 x 10^{-4} mM min^{-1} *versus* 1.9 x 10^{-6} mM min^{-1}, respectively) in accord with ps expectations. These data infer a role of microwave non-thermal factors in the photocatalytic reaction for the Vo-ST01 TiO_2 system, as in both cases the photodegradation was carried out under identical temperature conditions (100 °C). Non-thermal effects appear to play a role in pristine ST01, albeit to a lesser extent.

Microwave non-thermal factors seem to have had little consequence, if any, on the N-doped ST01 titania system, at least in the photodegradation of 2,4-D, as the data of **Table 2** and **Figure 7c** show that the degradation is faster under UV irradiation alone, and somewhat slower under both UV/MW and UV/CH irradiation conditions, albeit slightly faster under UV/MW in line with expectations from the picosecond data (**Table 1** and **Figure 6**).

4. Concluding remarks

Our *in-situ* examination of picosecond transient diffuse reflectance of three opaque titania samples while being microwave-irradiated has shown that microwaves had little influence on the ***fast*** decay kinetics of ***dry powders*** of pristine ST01 titania, oxygen-vacancy rich Vo-ST01 and N-doped ST01 systems, as the fast decay occurred within ca. 5 to 7 ns that we have attributed to recombination of free or shallow-trapped electrons with holes, while the ***slow*** decay for the ST01 and Vo-ST01 systems that occurred within about 0.30–0.40 μs and likely due to recombination of deeply-trapped electrons with (free or trapped) holes tended to be similar within experimental error. For the dry N-doped ST01 system, the ***slower*** decay was nearly twofold slower (3.1×10^6 s^{-1} (MW) *versus* 5.3×10^6 s^{-1} (MW)) when subjected to microwave irradiation. Significant differences were seen in the ***slow*** transient decay when the titania systems consisted of ***aqueous pastes***, particularly for the pristine ST01 and Vo-ST01 samples under microwave irradiation when compared to samples that were not MW-irradiated. Indeed, the ***slow*** decay occurred in >> 10 μs and 1.0 μs for these two systems, respectively, when MW-irradiated relative to 0.11 μs and 0.14 μs when not MW-irradiated. Microwave radiation likely causes either additional formation of defects that can trap electrons and/or change the trapping energies resulting in slower charge carrier recombination, a process that should enhance photocatalyzed reactions with these systems. Microwave non-thermal factors may have a role in affecting the electronic properties of titania. Such a role was evident in the photodegradation of the 2,4-D herbicide when comparing the dynamics between UV/MW and UV/CH irradiation under identical temperature conditions.

In accord with expectations from the ps results, the degradation of the 2,4-D herbicide in aqueous media was fastest under UV/MW irradiation than under UV/CH in both cases process occurring at 100 ^oC. Germane to the present study, Pan and coworkers[44] noted that oxygen vacancies play an important role in mediating interfacial electron transfer and so are expected to affect the photocatalytic activity of titania. Some researchers have noted that oxygen vacancies act as recombination centers of the photogenerated electrons with holes.[51] In this regard, Lin et al.[52] and Kitano and coworkers[53] contend that the concentration of oxygen vacancies likely reduces photocatalyst performance because as potential recombination centers they enhance recombination of the reductive and oxidative charge carriers. Our results show that under microwave irradiation charge carrier recombination was slower (i.e., longer decay times of the carriers), at least for the aqueous pastes of pristine ST01 and Vo-ST01 samples, and allowed reactions in aqueous media to be enhanced (under UV/MW vis-à-vis UV/CH) as they could compete more effectively with slower charge carrier recombination. Particularly significant were the results displayed in **Figure 7b** for the V_O-ST01 TiO_2 specimen for which we argue that the number of anion vacancies decreases in the order V_O-ST01-UV/CH > V_O-ST01-UV/MW > V_O-ST01; this infers that the lower the number of surface anion vacancies (and thus surface recombination centers) the greater should be the photoactivity of the titania specimen in line with the suggestion of Lin et al.[52] and Kitano and coworkers.[53] Microwave radiation, no doubt, likely imparts additional effects on titania specimens that have yet to be fully understood.

Acknowledgments

Financial support from the Japan Society for the Promotion of Science (JSPS) through a Grant-in-aid for Scientific Research (No. C-25420820), and from the Ministry of the Environment through the Environment Research and Technology Development Fund (Rehabilitation Adoption Budget) is gratefully appreciated. We are also grateful to the Sophia University-wide Collaborative Research Fund for a grant to S.H. This work was also partly supported by the Nanotechnology Platform Program (Advanced Characterization Nanotechnology Platform, A-13-AT-0034) of the Ministry of Education, Culture, Sports, Science and Technology (MEXT), Japan. A.V.E. is grateful to the Government of the Russian Federation for a Mega Grant (No. 14.Z50.31.0016) in support of the Project "Establishment of the Laboratory of Photoactive Nanocomposite Materials". N.S. thanks Prof. Albini of the University of Pavia (Italy) for his continued hospitality during the many winter semesters in his laboratory.

Notes and references

[a] Department of Material & Life Science, Faculty of Science and Technology, Sophia University, 7-1 Kioicho, Chiyodaku, Tokyo 102-8554, Japan. Email: horikosi@sophia.ac.jp
[b] Research Institute of Instrumentation Frontier (RIIF), National Institute of Advanced Industrial Science and Technology (AIST), 1-1-1 Umezono, Tsukuba, Ibaraki 305-8568, Japan.
[c] Laboratory of Photoactive Nanocomposite Materials, Saint-Petersburg State University, Ulianovskaia str. 1, Saint-Petersburg, 198504 Russian Federation.
[d] PhotoGreen Laboratory, Dipartimento di Chimica, Università di Pavia, Via Taramelli 12, Pavia 27100, Italy. Email: nick.serpone@unipv.it

† Electronic Supplementary Information (ESI) available: Original data from the picosecond transient diffuse reflectance spectroscopic study. See DOI: 10.1039/b000000x/

1 G. Rothenberger, J. Moser, M. Grätzel, N. Serpone and D.K. Sharma, Charge Carrier Trapping and Recombination Dynamics in Small Semiconductor Particles, *J. Am. Chem. Soc.* 1985**, 107,** 8054–8059.
2 J. Moser, M. Grätzel, D.K. Sharma and N. Serpone, Picosecond Time-Resolved Studies of Photosensitized Electron Injection in Colloidal Semiconductors, *Helv. Chim. Acta*, 1985, **68**, 1686-1690.
3 N. Serpone, D.K. Sharma, J. Moser and M. Grätzel, Reduction of Acceptor Relay Species by Conduction Band Electrons of Colloidal Titanium Dioxide. Light Induced Charge Separation in the Picosecond Time Domain, *Chem. Phys. Lett*., 1987, **136**, 47-51.
4 U. Kölle, J. Moser and M. Grätzel, M. Dynamics of Interfacial Charge-Transfer Reactions in Semiconductor Dispersions. Reduction of Cobaltocenium dicarboxylate in Colloidal TiO_2, *Inorg. Chem.* 1985, **24**, 2253–2258.
5 R. Howe and M. Grätzel, EPR Observation of Trapped Electrons in Colloidal Titanium Dioxide, *J. Phys. Chem.* 1985, **89**, 4495-4499.
6 A. Furube, T. Asahi, H. Masuhara, H. Yamashita and M. Anpo, Charge Carrier Dynamics of Standard TiO_2 Catalysts Revealed by Femtosecond Diffuse Reflectance Spectroscopy, *J. Phys. Chem. B* 1999, **103**, 3120-3127.
7 A. Furube, T. Asahi, H. Masuhara, H. Yamashita and M. Anpo, Direct Observation of Interfacial Hole Transfer from a Photoexcited TiO_2 Particle to an Adsorbed Molecule SCN^- by Femtosecond Diffuse Reflectance Spectroscopy**,** *Res. Chem. Intermed*. 2001, **27**, 177-187.
8 A. Furube, T. Asahi, H. Masuhara, H. Yamashita and M. Anpo, Direct Observation of a Picosecond Charge Separation Process in Photoexcited Platinum-Loaded TiO_2 Particles by Femtosecond Diffuse Reflectance Spectroscopy*, Chem. Phys. Lett*. 2001, **336**, 424-430.
9 A. Furube, T. Asahi, H. Masuhara, H. Yamashita and M. Anpo, Femtosecond Diffuse Reflectance Spectroscopy on Some Standard TiO_2Powder Catalysts*, Chem. Lett*. 1997, **26**, 735-736
10 M. Anpo and M. Takeuchi, The Design and Development of Highly Reactive Titanium Oxide Photocatalysts Operating under Visible Light Irradiation, *J. Catal*. 2003, **216**, 505–516.
11 W. Choi, A. Termin and M.R. Hoffmann, The Role of Metal Ion Dopants in Quantum-Sized TiO_2: Correlation between Photoreactivity and Charge Carrier Recombination Dynamics, *J. Phys. Chem.* 1994*,* **98**, 13669–13679.

12 D. Kuciauskas, J.E. Monat, R. Villahermosa, H.B. Gray, N.S. Lewis and J.K. McCusker, Transient Absorption Spectroscopy of Ruthenium and Osmium Polypyridyl Complexes Adsorbed onto Nanocrystalline TiO_2 Photoelectrodes, *J. Phys. Chem. B* 2002, **106**, 9347-9358.
13 D. Bahnemann, A. Henglein, J. Lilie and L. Spanhel, Flash Photolysis Observation of the Absorption Spectra of Trapped Positive Holes and Electrons in Colloidal TiO_2, *J. Phys. Chem.* 1984, **88**, 709-711.
14 D. Lawless, N. Serpone and D. Meisel, Semiconductor Photophysics. 6. The Role of OH radicals and Trapped Holes in Photocatalysis. A Pulse Radiolysis Study, *J. Phys. Chem.* 1991, **95**, 5166–5170.
15 R. Katoh, M. Murai and A. Furube, Transient Absorption Spectra of Nanocrystalline TiO_2 Films at High Excitation Density, *Chem. Phys. Lett*. 2010, **500**, 309–312. Y. Tamaki, A. Furube, M. Murai, K. Hara, R. Katoh and M. Tachiya, Dynamics of Efficient Electron–Hole Separation in TiO_2 Nanoparticles Revealed by Femtosecond Transient Absorption Spectroscopy under the Weak Excitation Condition, *Phys. Chem. Chem. Phys*. 2007, **9**, 1453–1460. T. Yoshihara, R. Katoh, A. Furube, Y. Tamaki, M. Murai, K. Hara, S. Murata, H. Arakawa and M. Tachiya, Identification of Reactive Species in Photoexcited Nanocrystalline TiO_2 Films by Wide-Wavelength-Range (400–2500 nm) Transient Absorption Spectroscopy, *J. Phys. Chem. B* 2004, **108**, 3817–3823.
16 H.G. Baldoví, B. Ferrer, M. Alvaro and H. García, Microsecond Transient Absorption Spectra of Suspended Semiconducting Metal Oxide Nanoparticles, *J. Phys. Chem. C* 2014, **118**, 9275−9282.
17 N. Serpone and E. Pelizzetti, (Eds.), Photocatalysis – Fundamentals and Applications, Wiley, New York, 1989.
18 A. Fujishima, K. Hashimoto and T. Watanabe, TiO_2 Photocatalysis – Fundamentals and Applications, BKC Publ., Tokyo, Japan, 1999.
19 X. Zhang, G. Li and Y. Wang, Microwave Assisted Photocatalytic Degradation of High Concentration Azo Dye Reactive Brilliant Red X-3B with Microwave Electrodeless Lamp as Light Source, *Dyes Pigments* 2007, **74**, 536–544.
20 G. Zhanqi, Y. Shaogui, T. Na and S. Cheng, Microwave Assisted Rapid and Complete Degradation of Atrazine Using TiO_2 Nanotube Photocatalyst Suspensions, *J. Hazard. Mater.* 2007, **145**, 424–430.
21 V. Cirkva, H. Žabvoa and M. Hajek, Microwave Photocatalysis of Monochloroacetic Acid over Nanoporous Titanium(IV) Oxide Thin Films Using Mercury Electrodeless Discharge Lamps, *J. Photochem. Photobiol. A* 2008, **198**, 13–17.
22 Z. Ai, P. Yang and X. Lu, Degradation of 4-Chlorophenol by a Microwave Assisted Photocatalysis method, *J. Hazard. Mater.* 2005, **124**, 147–152.
23 H. Zhong, Y. Shaogui, J. Yongming and S. Cheng, Microwave Photocatalytic Degradation of Rhodamine B Using TiO_2 Supported on Activated Carbon: Mechanism Implication, *J. Environ. Sci.* 2009, **21**, 268–272.
24 S. Horikoshi, M. Abe and N. Serpone, Influence of Alcoholic and Carbonyl Functions in Microwave-assisted and Photo-assisted Oxidative Mineralization, *Appl. Catal. B: Environ.* 2009, **89**, 284–287.
25 S. Horikoshi, H. Hidaka and N. Serpone, Hydroxyl Radicals in Microwave Photocatalysis. Enhanced Formation of OH Radicals Probed by ESR Techniques in Microwave-Assisted Photocatalysis in Aqueous TiO_2 Dispersions, *Chem. Phys. Lett*. 2003, **376**, 475–480.
26 S. Horikoshi, A. Matsubara, S. Takayama, M. Sato, F. Sakai, M. Kajitani, M. Abe and N. Serpone, Characterization of Microwave Effects on Metal-Oxide Materials: Zinc Oxide and Titanium Dioxide, *Appl. Catal. B: Environ*. 2009, **1**, 362–367.
27 S. Horikoshi, M. Kajitani and N. Serpone, The Microwave-/Photo-Assisted Degradation of Bisphenol-A in Aqueous TiO_2 Dispersions Revisited. Re-assessment of the Microwave Non-thermal Effect, *J. Photochem. Photobiol. A: Chem.* 2007, **188**, 1–4.
28 S. Horikoshi, Y. Minatodani, H. Sakai, M. Abe and N. Serpone, Characteristics of Microwaves on Second Generation Nitrogen-Doped TiO_2 Nanoparticles and their Effect on Photoassisted Processes, *J. Photochem. Photobiol., A: Chem.* 2011, **217**, 191–200.
29 S. Horikoshi, Y. Minatodani, H. Tsutsumi, H. Uchida, M. Abe and N. Serpone, Influence of Lattice Distortion and Oxygen Vacancies on the UV-Driven/Microwave-Assisted TiO_2 Photocatalysis, *J. Photochem. Photobiol., A: Chem.* 2013, **265**, 20–28.
30 K. Yanagisawa, Y. Yamamoto, Q. Feng and N. Yamasaki, Formation Mechanism of Fine Anatase Crystals from Amorphous Titania under Hydrothermal Conditions, *J. Mater. Res*. 1998, **13**, 825–829.
31 V.N. Kuznetsov and N. Serpone, Visible Light Absorption by Various Titanium Dioxide Specimens, *J. Phys. Chem. B* 2006, **110**, 25203–25209.
32 V.N. Kuznetsov and N. Serpone, On the Origin of the Spectral Bands in the Visible Absorption Spectra of Visible-Light-Active TiO_2 Specimens. Analysis and Assignments, *J. Phys. Chem. C* 2009, **113**, 15110−15123.
33 V.N. Kuznetsov, A.V. Emeline, A.V. Rudakova, M.S. Aleksandrov, N.I. Glazkova, V.A. Lovtcius, G.V. Kataeva, R.V. Mikhaylov, V.K. Ryabchuk and N. Serpone, Visible−NIR Light Absorption of Titania Thermochemically Fabricated from Titanium and its Alloys; UV- and Visible-Light- Induced Photochromism of Yellow Titania, *J. Phys. Chem. C* 2013, **117**, 25852− 25864.
34 V.N. Kuznetsov, V.K. Ryabchuk, A.V. Emeline, R.V. Mikhaylov, A.V. Rudakova and N. Serpone, Thermo- and Photo-stimulated Effects on the Optical Properties of Rutile Titania Ceramic Layers Formed on Titanium Substrates, *Chem. Mater*. 2013, **25**, 170−177
35 S. Horikoshi, F. Sakai, M. Kajitani, M. Abe, A.V. Emeline and N Serpone, Microwave-Specific Effects in Various TiO_2 Specimens. Dielectric Properties and Degradation of 4-Chlorophenol, *J. Phys. Chem. C* 2009, **113**, 5649–5657
36 A.V. Emeline, L.G. Smirnova, G.N. Kuzmin, L.L. Basov and N. Serpone, Spectral Dependence of Quantum Yields in Gas-Solid Heterogeneous Photosystems. Influence of Anatase/Rutile Content on the Photostimulated Adsorption of Dioxygen and Dihydrogen on Titania, *J. Photochem. Photobiol. A* 2002, **148**, 97–102.
37 A.V. Emeline, G.N. Kuzmin, D. Purevdorj, V.K. Ryabchuk and N. Serpone, Spectral Dependencies of the Quantum Yield of Photochemical Processes on the Surface of Wide Band Gap Solids. 3. Gas/Solid Systems, *J. Phys. Chem. B* 2000, **104**, 2989–2999.
38 A.V. Emeline, A. Salinaro and N. Serpone, Spectral Dependence and Wavelength Selectivity in Heterogeneous Photocatalysis. I. Experimental Evidence from the Photocatalyzed Transformation of Phenols, *J. Phys. Chem. B* 2000, **104**, 11202–11210.
39 N. Serpone, Is the Band Gap of Pristine TiO_2 Narrowed by Anion- and Cation-Doping of Titanium Dioxide in Second-Generation Photocatalysts?, *J. Phys. Chem. B* 2006, **110**, 24287– 24293.
40 T.-C. Lu, S.-Y. Wu, L.-B. Lin and W.-C. Zheng, Defects in the Reduced Rutile Single Crystal, *Physica B* 2001, **304**, 147–151.
41 A.V. Emeline, G.N. Kuzmin, L.L. Basov and N. Serpone, Photoactivity and Photoselectivity of a Dielectric Metal-Oxide Photocatalyst (ZrO_2) Probed by the Photoinduced Reduction of Oxygen and Oxidation of Hydrogen, *J. Photochem. Photobiol., A* 2005, **174**, 214–221. A.V. Emeline, A.V. Panasuk, N. Sheremetyeva and N. Serpone, Mechanistic Studies of the Formation of Different States of Oxygen on Irradiated ZrO_2 and the Photocatalytic Nature of Photoprocesses from Determination of Turnover Numbers, *J. Phys. Chem. B* 2005, **109**, 2785–2792. A.V. Emeline, G.V. Kataeva, A.S. Litke, A.V. Rudakova, V.K. Ryabchuk and N. Serpone, Spectroscopic and Photoluminescence Studies of a Wide Band Gap Insulating Material: Powdered and Colloidal ZrO_2 Sols, *Langmuir* 1998, **14**, 5011–5022.
42 N.S. Andreev, A.V. Emeline, V.A. Khudnev, S.A. Polikhova, V.K. Ryabchuk and N. Serpone, Photoinduced Chesorluminescence from Radical Processes on ZrO_2 Surfaces, *Chem. Phys. Lett*. 2000, **325**, 288–292.
43 E. Arcadipane, L. Romano, M. Zimbone, R. Sanz, G. Impellizzeri, M. A. Buccheri, M. Cantarella, M. Miritello, M.G. Grimaldi, V. Privitera, V. Quemener, C. Bhoodoo, P. Neuvonen, L. Vines, B. Svensson, TiO_2 nanostructures for applications in water purifications, *Proceedings of the 19th Conference on Semiconductor Photocatalysis and Solar Energy Conversion* (SPASEC-19), San Diego, CA, November 17-21, 2014.
44 X. Pan, M.-Q. Yang, X. Fu, N. Zhang and Y.-J. Xu, Defective TiO_2 with Oxygen Vacancies: Synthesis, Properties and Photocatalytic Applications, *Nanoscale* 2013, **5**, 3601–3614.
45 H.J. Kitchen, S.R. Vallance, J.L. Kennedy, N. Tapia-Ruiz, L. Carassiti, A. Harrison, A.G. Whittaker, T.D. Drysdale, S.W. Kingman and D.H. Gregory, Modern Microwave Methods in Solid-State Inorganic Materials Chemistry: From Fundamentals to Manufacturing, *Chem. Rev*. 2014, **114**, 1170−1206.
46 H. Nozaki and T. Iida, The Physical Properties of Titanium Oxide, Especially Electronic Structure of Coloring, *Seisan Kenkyu* 1964, **16**, 201−207.
47 N. Serpone, D. Lawless, R. Khairutdinov and E. Pelizzetti, Subnanosecond Relaxation Dynamics in TiO_2 Colloidal Sols (Particle Sizes R =

1.0–13.4 nm. Relevance to Heterogeneous Photocatalysis, *J. Phys. Chem.* 1995, **99**, 16655–16661.
48 A.V.Emeline, V.K. Ryabchuk, and N. Serpone, Factors Affecting the Efficiency of a Photocatalyzed Process in Aqueous Metal-Oxide Dispersions. Prospect for Distinguishing between the Two Kinetic Models, *J. Photochem. Photobiol. A: Chem.*, 2000, **133**, 89–96.
49 A.V. Emeline, N.V. Sheremetyeva, N.V. Khomchenko, V.K. Ryabchuk, and Serpone, Photoinduced formation of defects and nitrogen-stabilization of color centers in N-doped titanium dioxide, *J. Phys. Chem. C*, 2007, **111**, 11456–11462.;
50 C. Di Valentin, G. Pacchioni, A. Selloni, S. Livraghi, and E. Giamello, Characterization of Paramagnetic Species in N-Doped TiO_2 Powders by EPR Spectroscopy and DFT Calculations. *J. Phys. Chem. B*, 2005, **109**, 11414–11419.
51 J. Wang, D.N. Tafen, J.P. Lewis, Z. Hong, A. Manivannan, M. Zhi, M. Li and N. Wu, Origin of Photocatalytic Activity of Nitrogen-Doped TiO_2 Nanobelts, *J. Am. Chem. Soc.* 2009, **131**, 12290–12297.
52 Z. Lin, A. Orlov, R.M. Lambert and M.C. Payne, New Insights into the Origin of Visible Light Photocatalytic Activity of Nitrogen-Doped and Oxygen-Deficient Anatase TiO_2, *J. Phys. Chem. B* 2005, **109**, 20948–20952.
53 M. Kitano, M. Takeuchi, M. Matsuoka, J.M. Thomas and M. Anpo, Preparation of Visible Light- responsive TiO_2 Thin Film Photocatalysts by an RF Magnetron Sputtering Deposition Method and Their Photo-catalytic Reactivity, *Chem. Lett*. 2005, **34**, 616–617.

Graphical abstract